



A LETTERS JOURNAL EXPLORING  
THE FRONTIERS OF PHYSICS

OFFPRINT

## Random walk patterns of a soil bacterium in open and confined environments

M. THEVES, J. TAKTIKOS, V. ZABURDAEV, H. STARK and C. BETA

EPL, **109** (2015) 28007

Please visit the website  
[www.epljournal.org](http://www.epljournal.org)

**Note** that the author(s) has the following rights:

- immediately after publication, to use all or part of the article without revision or modification, **including the EPLA-formatted version**, for personal compilations and use only;
- no sooner than 12 months from the date of first publication, to include the accepted manuscript (all or part), **but not the EPLA-formatted version**, on institute repositories or third-party websites provided a link to the online EPL abstract or EPL homepage is included.

For complete copyright details see: <https://authors.eplletters.net/documents/copyright.pdf>.



# epl

A LETTERS JOURNAL EXPLORING  
THE FRONTIERS OF PHYSICS

## AN INVITATION TO SUBMIT YOUR WORK

[www.epljournal.org](http://www.epljournal.org)

### The Editorial Board invites you to submit your letters to EPL

EPL is a leading international journal publishing original, innovative Letters in all areas of physics, ranging from condensed matter topics and interdisciplinary research to astrophysics, geophysics, plasma and fusion sciences, including those with application potential.

The high profile of the journal combined with the excellent scientific quality of the articles ensures that EPL is an essential resource for its worldwide audience. EPL offers authors global visibility and a great opportunity to share their work with others across the whole of the physics community.

### Run by active scientists, for scientists

EPL is reviewed by scientists for scientists, to serve and support the international scientific community. The Editorial Board is a team of active research scientists with an expert understanding of the needs of both authors and researchers.



[www.epljournal.org](http://www.epljournal.org)

OVER  
**560,000**  
full text downloads in 2013

**24 DAYS**  
average accept to online  
publication in 2013

**10,755**  
citations in 2013

*"We greatly appreciate  
the efficient, professional  
and rapid processing of  
our paper by your team."*

Cong Lin  
Shanghai University

## Six good reasons to publish with EPL

We want to work with you to gain recognition for your research through worldwide visibility and high citations. As an EPL author, you will benefit from:

- 1 Quality** – The 50+ Co-editors, who are experts in their field, oversee the entire peer-review process, from selection of the referees to making all final acceptance decisions.
- 2 Convenience** – Easy to access compilations of recent articles in specific narrow fields available on the website.
- 3 Speed of processing** – We aim to provide you with a quick and efficient service; the median time from submission to online publication is under 100 days.
- 4 High visibility** – Strong promotion and visibility through material available at over 300 events annually, distributed via e-mail, and targeted mailshot newsletters.
- 5 International reach** – Over 2600 institutions have access to EPL, enabling your work to be read by your peers in 90 countries.
- 6 Open access** – Articles are offered open access for a one-off author payment; green open access on all others with a 12-month embargo.

Details on preparing, submitting and tracking the progress of your manuscript from submission to acceptance are available on the EPL submission website [www.epletters.net](http://www.epletters.net).

If you would like further information about our author service or EPL in general, please visit [www.epljournal.org](http://www.epljournal.org) or e-mail us at [info@epljournal.org](mailto:info@epljournal.org).

EPL is published in partnership with:



European Physical Society

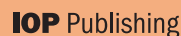


Società Italiana  
di Fisica

Società Italiana di Fisica



EDP Sciences



IOP Publishing

# Random walk patterns of a soil bacterium in open and confined environments

M. THEVES<sup>1</sup>, J. TAKTIKOS<sup>2,3</sup>, V. ZABURDAEV<sup>2,3</sup>, H. STARK<sup>2</sup> and C. BETA<sup>1(a)</sup>

<sup>1</sup> *University of Potsdam, Institute of Physics and Astronomy - Karl-Liebknecht-Str. 24/25, 14476 Potsdam, Germany*

<sup>2</sup> *Technical University of Berlin, Institute of Theoretical Physics - Hardenbergstr. 36, 10623 Berlin, Germany*

<sup>3</sup> *Max Planck Institute for the Physics of Complex Systems - Nöthnitzer Str. 38, 01187 Dresden, Germany*

received 6 August 2014; accepted in final form 14 January 2015  
published online 3 February 2015

PACS 87.17.Jj – Cell locomotion, chemotaxis

PACS 87.16.Qp – Pseudopods, lamellipods, cilia, and flagella

PACS 05.10.Gg – Stochastic analysis methods (Fokker-Planck, Langevin, etc.)

**Abstract** – We used microfluidic tools and high-speed time-lapse microscopy to record trajectories of the soil bacterium *Pseudomonas putida* in a confined environment with cells swimming in close proximity to a glass-liquid interface. While the general swimming pattern is preserved, when compared to swimming in the bulk fluid, our results show that cells in the presence of two solid boundaries display more frequent reversals in swimming direction and swim faster. Additionally, we observe that run segments are no longer straight and that cells swim on circular trajectories, which can be attributed to the hydrodynamic wall effect. Using the experimentally observed parameters together with a recently presented analytic model for a run-reverse random walker, we obtained additional insight on how the spreading behavior of a cell population is affected under confinement. While on short time scales, the mean square displacement of confined swimmers grows faster as compared to the bulk fluid case, our model predicts that for large times the situation reverses due to the strong increase in effective rotational diffusion.

Copyright © EPLA, 2015

**Introduction.** – Swimming constitutes the most prominent type of bacterial movement by which they explore a given environment during foraging in quest for food. It allows bacteria to direct their motion towards a chemical stimulus and spread towards more favorable habitats (chemotaxis) [1]. Swimming bacteria use the rotation of one or several helical filaments called flagella to propel themselves forward against the drag of the surrounding fluid. Each individual flagellum is anchored at the cell wall, where it is connected to a rotary motor unit, which can rotate in either clockwise (CW) or counterclockwise (CCW) direction [2]. In the presence of a solid-liquid interface, the speed of a swimming bacterium and the shape of its trajectory may change because of hydrodynamic interactions with the boundary [3]. Understanding bacterial swimming close to boundaries is important for the early aggregation phase of biofilm formation and processes of clinical infection [4,5].

A bacterium's swimming pattern critically depends on the number of flagella and on their arrangement across the cell body. The most prominent model organism *Escherichia coli* (*E. coli*) has several flagella that are randomly distributed across the cell body (peritrichous flagellation), see ref. [6] and references therein. Depending on the direction of rotation of the flagellar motors, flagella either form a synchronous bundle and the cell is said to execute a run, or they fly apart and the cell is said to undergo a tumble. Thus, the trajectory of a swimming cell displays alternating periods of almost straight, persistent displacement (runs) and reorientation events with small net displacement (tumble) [7]. In bacteria equipped with a single, polarly arranged flagellum (monotrichous flagellation) the swimming pattern is different. Depending on CW- or CCW-rotation of the motor, the cell alternates between a “forward” and a “backward” swimming mode. During the “forward” mode, the cell is swimming as a “pusher” with the cell body pointing towards the direction of propagation and the flagellum generating thrust

<sup>(a)</sup>E-mail: beta@uni-potsdam.de (corresponding author)

from behind. During the “backward” mode this situation is reversed and the cell is swimming as a “puller” with the flagellum now pointing towards the swimming direction. The corresponding trajectory of such a monoflagellated swimmer was shown to display a “zigzag” pattern where straight runs are interrupted by sharp reversals [8] but also more complicated variants have been observed [9].

Besides the well-studied cases of peritrichously and monotrichously flagellated bacterial swimmers described above, also intermediate cases are found, where several flagella are arranged in a polar tuft (lophotrichous flagellation). A prominent example is the soil bacterium *Pseudomonas putida* (*P. putida*) that is equipped with three to seven flagella polarly inserted at one end of the cell body [10]. We recently analyzed the motility statistics of *P. putida* in the bulk fluid [11]. In agreement with earlier studies [12], we found that the trajectories of *P. putida* display sharp turns, resembling the reversals in swimming direction reported for *V. alginolyticus*, with a strong peak in the turning angle distribution at an angle of around  $\psi \approx 180^\circ$  [9,11]. Remarkably, our analysis revealed that upon a reversal, the swimming speed of the cells on average changes by a factor of two. Based on existing theories [13], we developed a run-reverse random walk model with two alternating speeds of propagation to describe the spreading behavior of our cell population. With the experimentally observed values of mean runtime, rotational diffusion, and directional persistence we successfully recovered the long-term spreading and, in a refined version of the model, also the characteristics of the directional autocorrelation function for a population of free-swimming cells in the bulk fluid [11].

In its natural habitat, *P. putida* infects plant roots in a strongly confined porous soil environment. Previously, simulations have addressed the efficiency of a run-reverse random walk under frequent collisions with obstacles encountered in a porous medium [14]. In the present study, we used microfluidic tools to mimic a strongly confined environment and to investigate how the swimming pattern of *P. putida* is affected by the presence of solid boundaries. We furthermore demonstrate that our random walk model originally proposed for free-swimming cells in the bulk fluid can also be used to describe the diffusive spreading of a cell population in a confined environment.

**Experimental setup and data analysis.** – Analogously to [11], *Pseudomonas putida* *KT 2240* cells were grown from frozen stock in an overnight shaking solution of Lysogeny broth medium (LB-Medium Lennox, Applichem Darmstadt, Germany) with 10 g/L Tryptone, 5 g/L NaCl, 5 g/L Yeast extract and adjusted to  $pH \approx 7.0$ . From the stationary culture, 50  $\mu$ L of cell suspension was dispersed onto a solid LB-agar dish with 1.5% Agar-Agar and the dish was incubated for 24 hours at 30 °C. To achieve a pure culture, a loopful of cells was picked from the grown dish, transferred to a new agar dish and reincubated for another 24 hours. These stationary cell dishes containing

single colonies were constantly renewed and stored for a maximum of three weeks at 4 °C. In preparation of every motility experiment, a 50 mL flask with Nutrient-medium (N-Medium, 5 g/L Peptone, 3 g/L Meat extract, adjusted to  $pH \approx 7.0$ ) was inoculated by a single colony loop pick from the stationary dishes. Rotating at 300 rpm on a shaking culture at 30 °C, cells were grown overnight reaching stationary density. In the last step, the suspension was diluted with N-medium to an optical density of 0.05 (OD<sub>600</sub>, Eppendorf BioPhotometer Hamburg, Germany).

The diluted cell suspension, corresponding to a number density of approximately  $5 \cdot 10^7$  cells/mL, was filled into a microfluidic channel made from polydimethylsiloxane (PDMS) using soft lithography according to [15,16], measuring 30 mm in length, 525  $\mu$ m in width, and 10  $\mu$ m in height. Note that PDMS is oxygen permeable so that sufficient oxygen is available in our microfluidic channels to maintain a growing cell culture [17]. Cells quickly attached to the glass coverslip sealing the microchannel from below and started to grow by binary fission. This procedure was chosen since we found that, when grown beforehand in the shaking culture, due to the hydrophobic nature of the body, a majority of motile cells would attach to the channel walls and tubings during the filling procedure. Approximately six hours after the filling, a sufficient number of swimming cells populated the entire volume of the microchannel. Subsequently, the channel was mounted on the stage of an inverted microscope (Olympus IX-71, Tokyo, Japan). We then performed time-lapse recordings to follow the motion of swimming cells for a duration of one minute at a rate of 25 frames per second using an EoSens MC 1362/63 highspeed B/W camera (Mikrotron Munich, Germany). To ensure sufficient contrast, images were recorded with an Olympus 20X UPLFLN-PH phase contrast objective focused at the glass bottom of the microchannel. Due to the focal depth of this low magnification objective, we could monitor cell movement over the entire depth of the microchannel (10  $\mu$ m). Raw images with 1280  $\times$  1024 px were stored on a solid state disk and transferred to a Windows 7 personal computer.

Cells had an average size of  $4.78 \pm 0.08 \mu\text{m} \times 1.86 \pm 0.05 \mu\text{m}$ . The size was determined by analyzing 500 segmented images from our recording, each showing the contours of an average number of 230 cells. To segment the images and extract the cell centroid positions, a customized Matlab algorithm was written, see ref. [11] for details. With cell positions given at subsequent time intervals, the nearest-neighbor tracking algorithm by Crocker and Grier was then used to link positions together to form trajectories in time [18]. After the trajectories were smoothed using a running three-point average, speed and angular velocity were calculated from finite differences. The resulting cell trajectories showed the classical bacterial swimming pattern, where straight lines, corresponding to cells executing a run, are interrupted by sharp turning events. To distinguish between the two periods and to identify the turn events, another customized program was

used based on the algorithm by Masson *et al.* [19]. Local minima in swimming speed or in the absolute value of the angular velocity were considered as turn events, while all other parts of the trajectory were scored as a run, see ref. [11] for details.

Because we were looking at cells constantly swimming in close proximity to a surface, their motion and turn behavior can be affected by the presence of coexisting colonies on the surface. We therefore excluded from statistics all trajectories of cells passing or turning near a colony at a distance smaller than the average cell length ( $\sim 3 \mu\text{m}$ ). Additionally, we removed all trajectories of cells with an average speed below  $10 \mu\text{m/s}$  and with a displacement between the starting and ending point of the trajectory below  $3 \mu\text{m}$ . Our experimental data set then consisted of a total of 589 trajectories. To further exclude dead cells, dividing cells, or cells temporarily attached to the surface, another 185 trajectories were discarded after a visual inspection of every single trajectory. All motility statistics were then calculated from the remaining 404 trajectories of healthy cells.

**Results.** – In fig. 1, we show two different sample trajectories of cells swimming inside the confined microchannel. The trajectory in fig. 1(a) displays a zigzag-pattern of straight runs and frequent reversals in the swimming direction accompanied by alternating swimming speeds shown in (b). A second example is depicted in fig. 1(c). Here, the cell swims along circular paths, which is reflected by an increase in the average absolute angular velocity of the corresponding run segments shown in (d). While the trajectory in (a) displays a swimming pattern similar to the typical trajectory of a free-swimming cell in the bulk fluid, the curved runs of the second example in (c) can be attributed to a wall-induced hydrodynamic effect acting on cells that swim in close proximity to a solid boundary (see the Discussion below for further details).

The distribution of turning angles in fig. 2(a) shows a dominant peak at  $\psi \approx 180^\circ$ , clearly demonstrating that in most cases (eight out of ten), runs are interrupted by reversals in the swimming direction. To a lesser extent, also turning events are observed, where the direction of propagation undergoes only moderate changes, reflected by a small second maximum at  $\psi \approx 0^\circ$ .

In the following, analogous to our analysis of cells swimming in the bulk fluid [11], we restricted our analysis to cells displaying reversal events only, which accounted for 248 out of a total number of 404 trajectories with an average trajectory length of 3.8 s. For those we calculated a directional persistence parameter  $\alpha = \langle \cos \psi \rangle = -0.98$ . To investigate systematic changes in the swimming speed we plot the distribution of differences in speed before and after a reversal normalized by the sum of both speeds  $Q = (v_{k+1} - v_k)/(v_{k+1} + v_k)$  in fig. 2(b). Two peaks at  $Q \approx \pm 0.25$  are observed indicating that upon a reversal, cells indeed change their swimming speed by a factor of approximately 1.7 on average. The distribution of

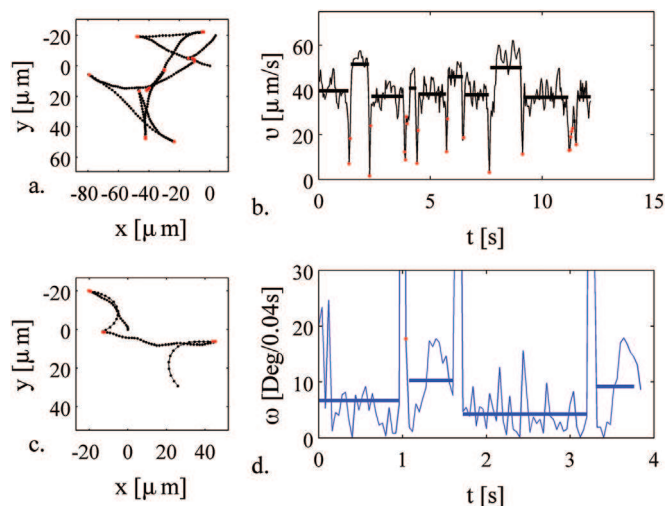


Fig. 1: (Colour on-line) Sample trajectories of cells swimming in a microchannel measuring  $10 \mu\text{m}$  in height. Runs (black dots) are interrupted by reversals in swimming direction (red dots). (a) Trajectory of a cell swimming stepwise along a line. (b) Upon a reversal, the cell systematically changes its average swimming speed. (c) Trajectory of a cell swimming near the channel boundary. (d) Interrupted by reversals, the cell alternates between runs with higher and lower curvature as reflected by the angular velocity of the corresponding cell. However, no systematic trend between successive average run angular velocities was observed, see fig. S2 in the Supplementary Material at [http://www.bio.physik.uni-potsdam.de/supplement\\_theves.pdf](http://www.bio.physik.uni-potsdam.de/supplement_theves.pdf).

run speeds is shown in fig. 2(c). Using a double Gaussian fit, we were able to estimate the two average swimming speeds to  $v_1 = 30.8 \mu\text{m/s}$  and  $v_2 = 49.9 \mu\text{m/s}$  with the corresponding standard deviations  $\sigma_1 = 8.2 \mu\text{m/s}$  and  $\sigma_2 = 7.0 \mu\text{m/s}$ .

The runs are not perfectly straight lines. Thermal agitation and intrinsic noise from the propulsion mechanism continuously induce small fluctuations in the swimming direction. Additionally, hydrodynamic wall effects may generate a torque that acts on the cell body and leads to a strongly curved trajectory, see fig. 1(c) for example. While the former effect on the swimming direction is random, the hydrodynamic wall effect constitutes a deterministic force acting on the trajectory of a moving cell. The magnitude of this force depends on the distance of the swimming cell to the upper or lower channel boundary and we observe a distribution of different average curvature radii and signs during a run, see fig. 3(a). Because the distribution is centered at zero and we equally often observe positive and negative curvature signs corresponding to trajectories describing a clockwise or counterclockwise circle, we may approximate both effects acting on the swimming direction by an effective rotational diffusion constant. From a single exponential fit to the directional autocorrelation function calculated from the run segments of the trajectories, we determined an effective rotational diffusion constant

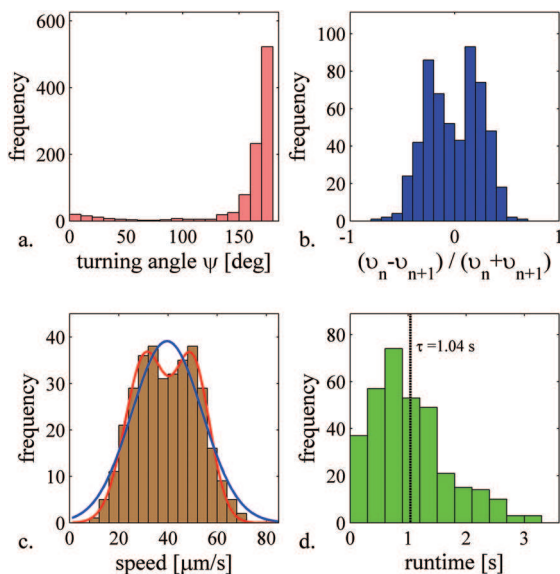


Fig. 2: (Colour on-line) (a) Frequency distribution of turning angles. (b) Distribution of  $Q = (v_{k+1} - v_k)/(v_{k+1} + v_k)$ , the difference in average speed before and after a reversal divided by the sum of average speeds. Two peaks around  $\pm 0.25$  are observed. (c) Distribution of run speeds. Cells swim with an average speed of  $v = 39.6 \mu\text{m/s}$ , determined from the mean value of a Gaussian fit (blue line). The shape of the distribution can be also approximated by a superposition of two Gaussians, yielding  $v_1 = 30.8 \mu\text{m/s}$  and  $v_2 = 49.9 \mu\text{m/s}$  (red line), which indicates a bimodal behavior of the cell speed. (d) Distribution of runtimes with an average runtime  $\langle \tau \rangle = 1.04$  s.

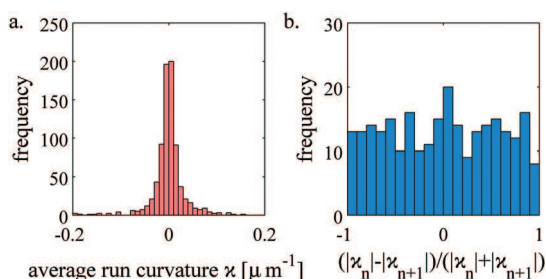


Fig. 3: (Colour on-line) (a) Distribution of average curvatures of all run segments from experimental cell trajectories. The distribution is centered at zero. With equal probability cells in the confined environment swim on right or left curved paths with varying curvature magnitude. (b) Frequency distribution of differences in curvature magnitude upon a reversal normalized by the two magnitudes. There is no indication for a systematic change in curvature sign or magnitude upon a reversal.

$D_r = 0.091 \text{ rad}^2/\text{s}$ , see fig. 4(a). Furthermore, we found no systematic changes in curvature magnitude upon a reversal, see fig. 3(b).

Finally, the distribution of runtimes calculated from trajectories with reversal events only is given in fig. 2(d). We observe a local maximum around 0.7 s and an exponential tail for larger times. The average runtime is given by the mean value of the experimentally derived runtimes,  $\tau = 1.04$  s. In a first approximation, we assume that the

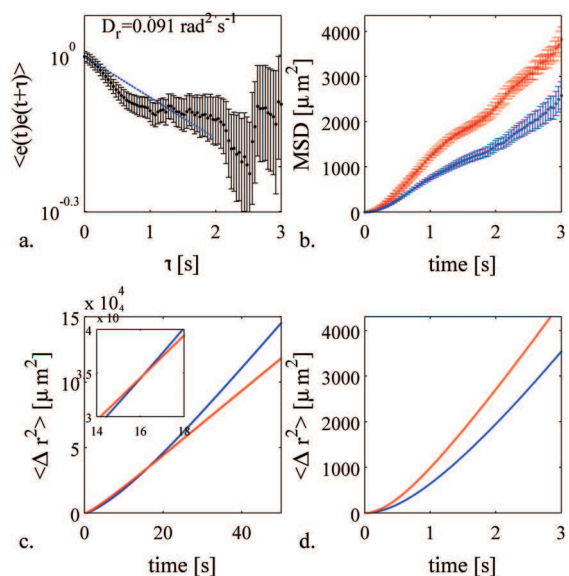


Fig. 4: (Colour on-line) (a) Directional autocorrelation computed from runs only. A single exponential fit  $\langle \mathbf{e}(0) \cdot \mathbf{e}(t) \rangle_{\text{runs}} = e^{-2D_r t}$  was used to derive the rotational diffusion constant from the experimental data. (b) Mean square displacement (MSD). Experimental data for cells swimming in a confined microchannel (red) are shown together with results for free-swimming cells in the bulk fluid (blue) taken from ref. [11]. Bars display the mean squared error (MSE). (c) Theoretical predictions on MSD for cells in confinement (red) and bulk fluid (blue) based on the analytic model with parameters taken from table 1. (d) Theoretical prediction from the same analytic expression but now for shorter time scales. See text for closer description.

distribution of runtimes follows Poisson statistics resulting in an exponential distribution that allows for analytical solutions of our random walk model presented in [11] and used below.

**Discussion.** – Using microfluidic tools, we have analyzed the swimming behavior of the soil bacterium *P. putida* under confinement, in the presence of two solid boundaries a distance of  $10 \mu\text{m}$  apart. In table 1, our experimental results are summarized together with the corresponding data for free-swimming cells in the bulk fluid from ref. [11]. Note that in ref. [11], we restricted our analysis to trajectories that lie in a narrow zone of  $\pm 7 \mu\text{m}$  around the focal plane. This was achieved by excluding trajectories that were slower than  $10 \mu\text{m/s}$  and shorter than 2 s. The present data that was recorded in a  $10 \mu\text{m}$  deep microchannel can thus be directly compared to the data from ref. [11] — in both cases, we analyze 2D projections of trajectories that lie in a quasi-2D slice of  $10\text{--}14 \mu\text{m}$  thickness; in the present data, the slice is bounded by solid walls, as compared to the data in Theves *et al.* 2013, where there were no walls.

Compared to the bulk fluid case, the run-reverse pattern is generally preserved in the confined environment with a strong peak in the turning angle distribution around  $\psi \approx 180^\circ$  and a similar persistence parameter  $\alpha$ . Also

Table 1: Comparison of parameters calculated from cell trajectories in the bulk fluid [11] and in the 10  $\mu\text{m}$  microchannel. The first row shows the ratio between the number of reversal events,  $n_r$ , and the total number of turning events  $n$ .

Description	Parameter	Bulk fluid	Confined
reversals/turns	$n_r/n$	0.67	0.86
persistence prm.	$\alpha$	-0.95	-0.98
runspeed 1	$v_1$ ( $\mu\text{m/s}$ )	19.4	30.8
runspeed 2	$v_2$ ( $\mu\text{m/s}$ )	38.3	49.9
runtime	$\tau$ (s)	1.50	1.04
rotational diffusion constant	$D_r$ ( $\text{rad}^2/\text{s}$ )	0.023	0.091

pausing events with a turning angle of  $\psi \approx 0^\circ$  are observed, in agreement with a recent analysis based on a tethering assay [20]. Additionally, like in the bulk fluid, we observed a systematic change in swimming speed upon a reversal by a constant factor. While the total swimming speed is 30% higher than in the bulk fluid, the difference between the two distinct swimming speeds is less pronounced under confinement with  $v_2/v_1 \approx 1.7$  on average for the trajectories in the microchannel compared to  $v_2/v_1 \approx 2.0$  for the free-swimming cells. The average runtime, *i.e.* the time between reversal events, is smaller in the confinement (1.04s as compared to 1.50s). This may indicate a destabilization of the flagellar bundle by steric interactions with the channel walls. Because cells in the microchannel swim faster, however, the average run length is comparable. In both cases, the cells swim over a distance of 40–45  $\mu\text{m}$  before entering a new reversal event. Compared to the free-swimming case, the *effective* rotational diffusion under confinement is strongly enhanced and about four times larger than in the bulk fluid ( $D_r = 0.091 \text{ rad}^2/\text{s}$  as compared to  $D_r = 0.023 \text{ rad}^2/\text{s}$ ). Clearly, this can be attributed to a significant number of cells swimming on curved trajectories similar to the one displayed in fig. 1(c).

Our observations of circular trajectories are in agreement with earlier experiments and can be attributed to a hydrodynamic wall effect [21]. In the presence of a solid boundary, the rotational drag acting on the lower half of the cell body and flagellar bundle is stronger than on the upper half further away from the boundary. Because both cell body and flagellar bundle are rotating in opposing directions, the resulting asymmetry induces a torque which leads the cell to describe a curved trajectory [3,22]. The strong increase in average swimming speed, however, cannot be explained by the existing theories. Numerical and analytical solutions based on resistive force theory are available and they predict a 10–30% increase in swimming speed only at distances  $d \approx 10\text{--}100 \text{ nm}$  away from the boundary [21,23]. To account for hydrodynamic interactions with the boundary at distances larger than the

cell size, a microswimmer has been described by a linear combination of fundamental solutions of the Stokes equation, in leading order by a positive force dipole [24]. Except for cells swimming at large inclination angles with respect to a surface, which we can rule out for our experiment, no increase in swimming speed was predicted. Note that hydrodynamic interactions may lead to an inhomogeneous distribution of cells between the bulk fluid and the regions close to surfaces because of differences in size and swimming speed [25]. To rule out a possible bias in our cell population, we determined the average size of swimming cells as a function of distance from the surface of a larger chamber, like the one used in ref. [11]. No difference between cells swimming close to the surface or far away from the surface was found, suggesting that the two populations can be safely compared to each other, see fig. S1 in the Supplementary Material at <http://www.bio.physik.uni-potsdam.de/supplement.theves.pdf>.

In fig. 4(b) we display the mean square displacement (MSD) as a function of time for *P. putida* cells swimming in a microchannel with 10  $\mu\text{m}$  in height together with the corresponding result for free-swimming *P. putida* cells taken from ref. [11]. The MSD was determined by averaging over the individual values from all trajectories with sufficient length. On the time scale of our experiment,  $t < 3 \text{ s}$ , cells swimming under confinement showed a faster effective diffusion than free-swimming cells. Based on our model that describes a run-reverse random walker with two alternating swimming speeds presented in [11], we were able to derive an analytic expression for the effective diffusion constant at large times ( $D = \lim_{t \rightarrow \infty} \langle [\mathbf{r}(t) - \mathbf{r}(0)]^2 \rangle / 6t$ ),

$$D = \frac{2D_R(v_1^2 + v_2^2) + \lambda(v_1^2 + v_2^2 + 2\alpha v_1 v_2)}{6[2D_R + \lambda(1 - \alpha)][2D_R + \lambda(1 + \alpha)]}. \quad (1)$$

With values taken from experimental data as listed in table 1, this expression yields

$$\frac{D_{conf}}{D_{bulk}} \approx \frac{411 \mu\text{m}^2/\text{s}}{581 \mu\text{m}^2/\text{s}} \approx 0.71. \quad (2)$$

This seems to contradict our experimental data, where we observed a faster spreading under confinement. Note, however, that eq. (1) for the diffusion constant  $D$  was derived for the limit of large times, whereas our experimental data only extends over a duration of 3s. If we consider the *full* analytic expression for the MSD as a function of time with parameters for confinement and bulk taken from experiments, we observe that the two curves cross each other at  $t_c \approx 16 \text{ s}$ , see fig. 4(c) (see the Supplementary Material at <http://www.bio.physik.uni-potsdam.de/supplement.theves.pdf> and the supplementary Mathematica script with the full formula for the MSD at <http://www.bio.physik.uni-potsdam.de/Formula.MSD.full.nb>). Below  $t_c$ , we find qualitative agreement with the trend in the experimental data shown in fig. 4(b). Here, the MSD increases faster for the confined swimmers. However, above  $t_c$ , the

situation reverses. For large times, the free swimmers explore their environment faster than the cells swimming in a confined environment in agreement with eq. (2), see fig. 4(d). Note that in general, the analytic results derived in ref. [11] hold for arbitrary dimensions.

It is currently not clear how the multiple, polar flagella of *P. putida* reorient during a reversal event. To clarify this mechanism, high-speed fluorescence microscopy recordings of the flagellar dynamics are required [7,26]. To date, these recordings could not be successfully completed due to phototoxic effects on the flagellar motor. Future efforts shall concentrate on indirect approaches like imaging of the flow field around a cell using tracer particles [27] or tracking of fluorescent nanobeads attached to the flagellar filaments [28].

In conclusion, while the flagellar mechanism of the reversal events remains elusive, we provide a detailed understanding of how populations of *P. putida* spread in a confined environment. On short time scales, the MSD of the confined swimmers grows faster than the MSD of free-swimming cells, due to their faster swimming speed. For larger times, however, the analytical model predicts that confined cells diffuse slower, dominated by the strongly enhanced rotational diffusion and the smaller difference in the two propagation speeds. Due to the finite focal depth and the limited measurement times, this regime is not accessible with our current experimental tools. However with future improvements on our setup, we hope to be able to experimentally verify the predicted crossover in the time evolution of the MSD of confined and freely swimming bacteria.

\*\*\*

Financial support of the Deutsche Forschungsgemeinschaft through GRK 1558 is gratefully acknowledged.

## REFERENCES

- [1] MADIGAN M. T., MARTINKO J. M., STAHL D. A. and CLARK D. P., *Brock Biology of Microorganisms* (Addison-Wesley Longman) 2011.
- [2] BERG H. C., *Annu. Rev. Biochem.*, **72** (2003) 19.
- [3] LAUGA E. and POWERS T. R., *Rep. Prog. Phys.*, **72** (2009) 096601.
- [4] COSTERTON J. W., STEWART P. S. and GREENBERG E. P., *Science*, **284** (1999) 1318.
- [5] DONLAN R. M. and COSTERTON J. W., *Clin. Microbiol. Rev.*, **15** (2002) 167.
- [6] BERG H., *E.coli in Motion* (Springer) 2004.
- [7] DARNTON N. C., TURNER L., ROJEVSKY S. and BERG H. C., *J. Bacteriol.*, **189** (2007) 1756.
- [8] JOHANSEN J. E., PINHASSI J., BLACKBURN N., ZWEIFEL U. L. and HAGSTRÖM A., *Aquat. Microb. Ecol.*, **28** (2002) 229.
- [9] XIE L., ALTINDAL T., CHATTOPADHYAY S. and WU X.-L., *Proc. Natl. Acad. Sci. U.S.A.*, **108** (2011) 2246.
- [10] HARWOOD C. S., FOSNAUGH K. and DISPENZA M., *J. Bacteriol.*, **171** (1989) 4063.
- [11] THEVES M., TAKTIKOS J., ZABURDAEV J., STARK H. and BETA C., *Biophys. J.*, **105** (2013) 1915.
- [12] DUFFY K. J. and FORD R. M., *J. Bacteriol.*, **179** (1997) 1428.
- [13] LOVELY P. S. and DAHLQUIST F. W., *J. Theor. Biol.*, **50** (1975) 477.
- [14] DUFFY K. J., CUMMINGS P. T. and FORD R. M., *Biophys. J.*, **68** (1995) 800.
- [15] XIA Y. and WHITESIDES G. M., *Annu. Rev. Mater. Sci.*, **28** (1998) 153.
- [16] DUFFY D. C., McDONALD J. C., SCHUELLER O. J. A. and WHITESIDES G. M., *Anal. Chem.*, **70** (1998) 4974.
- [17] RAO H.-X. and ZHANG Z. Y., *Annu. Rev. Mater. Sci.*, **303** (2007) 132.
- [18] CROCKER J. C. and GRIER D. G., *J. Colloid Interface Sci.*, **179** (1996) 298.
- [19] MASSON J. B., VOISSINE G., WONG-NG J., CELANI A. and VERGASSOLA M., *Proc. Natl. Acad. Sci. U.S.A.*, **109** (2012) 1802.
- [20] QIAN C., WONG C. C., SWARUP S. and CHIAM K.-H., *Appl. Environ. Microbiol.*, **79** (2013) 4734.
- [21] LAUGA E., DiLUZIO W. R., WHITESIDES G. M. and STONE H. A., *Biophys. J.*, **90** (2006) 400.
- [22] NAKAI T., KIKUDA M., KURODA Y. and GOTO T., *J. Biomech. Sci. Eng.*, **4** (2009) 2.
- [23] RAMIA M., TULLOCK D. L. and PHAN-THIEN N., *Biophys. J.*, **65** (1993) 755.
- [24] SPAGNOLIE S. E. and LAUGA E., *J. Fluid Mech.*, **700** (2012) 105.
- [25] BERKE A. P., TURNER L., BERG H. C. and LAUGA E., *Phys. Rev. Lett.*, **101** (2008) 038102.
- [26] TURNER L., RYU W. S. and BERG H. C., *J. Bacteriol.*, **182** (2000) 2793.
- [27] DRESCHER K., DUNKEL J., CISNEROS L. H., GANGULY S. and GOLDSTEIN R. E., *Proc. Natl. Acad. Sci. U.S.A.*, **108** (2011) 10940.
- [28] NAKAMURA S., KAMI-IKE N., YOKOTA J. P., MINAMINO T. and NAMBA K., *Proc. Natl. Acad. Sci. U.S.A.*, **107** (2010) 17616.